



## OPEN ACCESS

## EDITED BY

Alexey V. Glukhov,  
University of Wisconsin-Madison,  
United States

## REVIEWED BY

Xianwei Zhang,  
University of California, Davis,  
United States  
Seth H. Weinberg,  
The Ohio State University, United States  
Tim De Coster,  
Leiden University Medical Center (LUMC),  
Netherlands

## \*CORRESPONDENCE

Yael Yaniv,  
✉ yanivyael@gmail.com

†These authors have contributed equally  
to this work

RECEIVED 30 May 2023

ACCEPTED 03 July 2023

PUBLISHED 17 July 2023

## CITATION

Keidar N, Peretz NK and Yaniv Y (2023),  
Ca<sup>2+</sup> pushes and pulls energetics to  
maintain ATP balance in atrial cells:  
computational insights.  
*Front. Physiol.* 14:1231259.  
doi: 10.3389/fphys.2023.1231259

## COPYRIGHT

© 2023 Keidar, Peretz and Yaniv. This is an  
open-access article distributed under the  
terms of the [Creative Commons  
Attribution License \(CC BY\)](https://creativecommons.org/licenses/by/4.0/). The use,  
distribution or reproduction in other  
forums is permitted, provided the original  
author(s) and the copyright owner(s) are  
credited and that the original publication  
in this journal is cited, in accordance with  
accepted academic practice. No use,  
distribution or reproduction is permitted  
which does not comply with these terms.

# Ca<sup>2+</sup> pushes and pulls energetics to maintain ATP balance in atrial cells: computational insights

Noam Keidar<sup>†</sup>, Noa Kirschner Peretz<sup>†</sup> and Yael Yaniv<sup>\*</sup>

Laboratory of Bioenergetic and Bioelectric Systems, Biomedical Engineering Faculty, Technion-Israel Institute of Technology (IIT), Haifa, Israel

To maintain atrial function, ATP supply-to-demand matching must be tightly controlled. Ca<sup>2+</sup> can modulate both energy consumption and production. In light of evidence suggesting that Ca<sup>2+</sup> affects energetics through “push” (activating metabolite flux and enzymes in the Krebs cycle to push the redox flux) and “pull” (acting directly on ATP synthase and driving the redox flux through the electron transport chain and increasing ATP production) pathways, we investigated whether both pathways are necessary to maintain atrial ATP supply-to-demand matching. Rabbit right atrial cells were electrically stimulated at different rates, and oxygen consumption and flavoprotein fluorescence were measured. To gain mechanistic insight into the regulators of ATP supply-to-demand matching in atrial cells, models of atrial electrophysiology, Ca<sup>2+</sup> cycling and force were integrated with a model of mitochondrial Ca<sup>2+</sup> and a modified model of mitochondrial energy metabolism. The experimental results showed that oxygen consumption increased in response to increases in the electrical stimulation rate. The model reproduced these findings and predicted that the increase in oxygen consumption is associated with metabolic homeostasis. The model predicted that Ca<sup>2+</sup> must act both in “push” and “pull” pathways to increase oxygen consumption. In contrast to ventricular trabeculae, no rapid time-dependent changes in mitochondrial flavoprotein fluorescence were measured upon an abrupt change in workload. The model reproduced these findings and predicted that the maintenance of metabolic homeostasis is due to the effects of Ca<sup>2+</sup> on ATP production. Taken together, this work provides evidence of Ca<sup>2+</sup> “push” and “pull” activity to maintain metabolic homeostasis in atrial cells.

## KEYWORDS

atria, energetic balance, ATP, computational modeling, ATP supply

## 1 Introduction

The atria conduct the electrical activity from the sinoatrial node to the heart's ventricles and both passively and actively enhance ventricular diastolic filling. High and rapidly fluctuating metabolic rates are necessary to perform these electrical and mechanical tasks (Balaban, 2012), thus ATP supply-to-demand matching is crucial. Although mechanisms that match ventricular ATP supply to demand have been

**Abbreviation:** AF, Atrial fibrillation; ATP, Adenosine triphosphate; Ca<sup>2+</sup>m, Mitochondrial calcium; CK, Creatine kinase; PDH, Pyruvate dehydrogenase; SR, Sarcoplasmic reticulum.

investigated since the early 1950s, the identity and the specific targets of the control mechanisms, even under normal conditions, remain controversial (Yaniv et al., 2010). In addition, regulation of atrial energetics is not well understood.

Mitochondria are the main producers of ATP in atrial cells, and both  $\text{Ca}^{2+}$  and ADP have been suggested as key regulators of matching respiratory to energy supply to varying demands (Mason et al., 2020); yet their targets remain to be determined (Liberopoulos, 2013). ADP activates enzymes in the Krebs cycle, and thereby “pushes” the respiratory flux toward ATP generation (Harris and Das, 1991). In parallel, ADP controls ATP synthase by its availability, and thereby “pulls” ATP production by increasing respiratory flux (Chance and Williams, 1955). Activation of ATP synthase facilitates redox flux through the electron transport chain and increases ATP production. While  $\text{Ca}^{2+}$  is generally thought to act as a “push” control over ATP production (Harris and Das, 1991), by activating metabolite flux and enzymes in the Krebs cycle to push the redox flux, accumulating evidence suggests its role as a “pull” regulator (Territo et al., 2000). Whether  $\text{Ca}^{2+}$  control of metabolism works via both “pull” and “push” mechanisms in atrial cells under physiological conditions is not known. Moreover, while metabolic homeostasis in response to increased workload was shown in the heart (Balaban, 2012), it remains to be determined whether it is maintained in atrial cells in response to electrical stimulation.

To gain mechanistic insights into the regulators of such matching in atrial cells, this work constructed a computer model that integrated models of electrophysiology (Lindblad et al., 1996),  $\text{Ca}^{2+}$  cycling (Lindblad et al., 1996; Aslanidi et al., 2009) and force (Yaniv et al., 2006), to describe ATP demand, with a model of mitochondrial  $\text{Ca}^{2+}$  (Nguyen et al., 2007) and a modified model of mitochondrial energy metabolism (Cortassa et al., 2006). The integrated model was validated by conducting experiments measuring oxygen consumption and flavoprotein activity in response to increased electrical stimulation rates.

We hypothesized that: i)  $\text{Ca}^{2+}$  is an important regulator of ATP supply-to-demand matching, ii)  $\text{Ca}^{2+}$  both “pulls” and “pushes” ATP production and iii) metabolic homeostasis is maintained in atrial cells during increased electrical stimulation or abrupt changes in workload.

By combining experimental and computational results, we found ATP supply only matched the demand when  $\text{Ca}^{2+}$  both “pulled” and “pushed” ATP. Moreover, no rapid time-dependent changes in mitochondrial flavoprotein fluorescence level were observed in response to an abrupt change in workload, due to  $\text{Ca}^{2+}$  ion regulation of cell bioenergetics.

## 2 Materials and methods

### 2.1 Animal use

Animals were treated in accordance with the Technion Ethics Committee. The experimental protocols were approved by the Animal Care and Use Committee of the Technion (Ethics numbers: IL-118-10-13 and IL-001-01-19).

### 2.2 Atrial cell isolation

Hearts were isolated from healthy male New Zealand white rabbits weighing 2.3–2.7 kg. Each rabbit was weighed and then sedated with an intramuscular injection of ketamine (0.1 ml/kg) and xylazine (0.1 ml/kg). An intravenous cannula was inserted in the rabbit's ear for delivery of 200 mg/ml sodium pentobarbital diluted with heparin. The adequacy of the anesthesia was evaluated by observing the loss of reflexes in the eye and foot. The atrial cell isolation procedure is described in (Kirschner Peretz et al., 2017).

### 2.3 Cytosolic $\text{Ca}^{2+}$ measurements

$\text{Ca}^{2+}$  cycling into and out of the atrial cell cytosol was measured with Fluo-4 AM (ThermoFisher Scientific), as previously described (Davoodi et al., 2017). Data from (Davoodi et al., 2017; Kirschner Peretz et al., 2017) were reanalyzed on a custom-made guided user interface (GUI) programmed in MATLAB (Davoodi et al., 2017).

### 2.4 Electrical stimulation

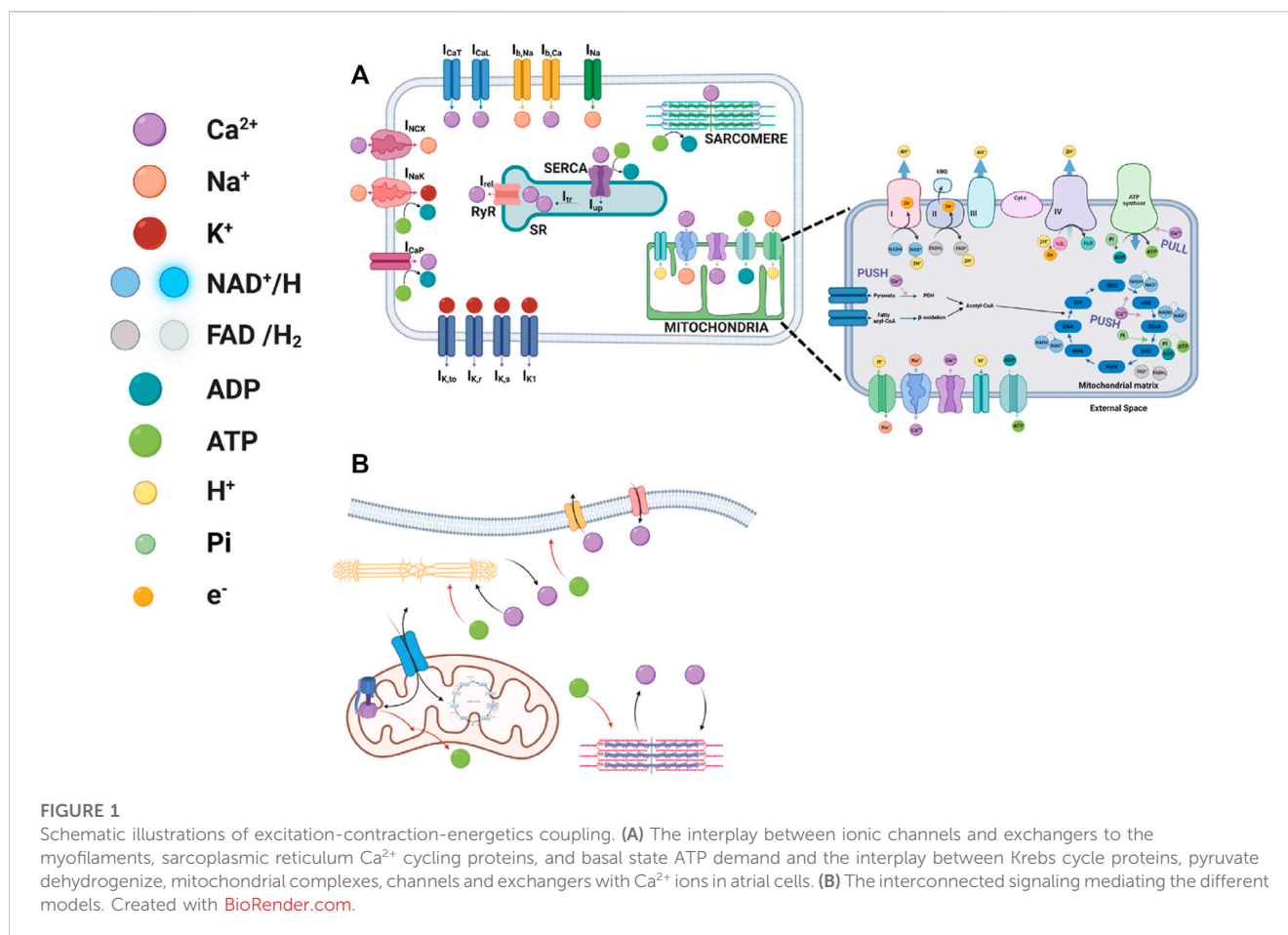
Cytosolic  $\text{Ca}^{2+}$  dynamics, flavoprotein autofluorescence and oxygen consumption following electrical stimulation at 1–3 Hz were measured. Electrical fields were created by a pair of platinum electrodes (0.008”bare wire, A-M Systems) glued to a custom-made chamber top.

### 2.5 Flavoprotein autofluorescence measurements

The autofluorescence of mitochondrial flavoprotein of atrial cells was imaged, at different electrical stimulation frequencies (quiescent, 0.25, 1, 2, and 3 Hz), at  $37^{\circ}\text{C} \pm 0.5^{\circ}\text{C}$ , under an inverted fluorescence microscope (Zeiss Observer Z1) with a 40x/1.4 N.A oil immersion lens and a 445 nm light-emitting diode (LED). Images were captured at 2 frames per second.

### 2.6 Oxygen consumption

Oxygen consumption by either quiescent or electrically stimulated (1, 2 or 3 Hz) atrial cell suspensions was measured using Clark-type electrodes (MT200, Strathkelvin Instruments Ltd.). For the oxygen chamber, a custom-sealed plunger that included platinum wires was designed, as previously described (Yaniv et al., 2011). Atrial cell suspensions were centrifuged at 1000 RPM for 10 min, and the supernatant was aspirated. The resuspended cells were incubated in fresh HEPES solution containing (in mM): NaCl 140, KCl 5.4, HEPES 5, glucose 10,  $\text{MgCl}_2$  2, and  $\text{CaCl}_2$  1 (pH 7.4 with NaOH). The cell suspension was divided into two equal aliquots, one of which was subjected to electrical stimulation and the second served as a control. The atrial cell suspensions were stirred gently under quiescent conditions in HEPES buffer for 2 min at  $36^{\circ}\text{C}$ , and then electrically stimulated at 1, 2 and 3 Hz for 1 min and again maintained under quiescent



conditions for 1 min. Following measurement of oxygen consumption, total protein concentration (BCA™ Protein Assay) and the number of viable cells in the cell suspension were determined. Oxygen consumption of the atrial cells was normalized to the protein concentration.

## 2.7 Statistics

All experiments were performed on cells from at least three rabbits. All data are presented as mean  $\pm$  SD. Comparisons were made using a one-way repeated measurement ANOVA test with  $p < 0.05$  taken to indicate statistical significance.

## 2.8 The numerical model general approach

The model describing the atrial membrane potential, ionic currents,  $\text{Ca}^{2+}$  cycling, force generation and energetics (Figure 1A) was based on rabbit atrial excitation-contraction modeling (Lindblad et al., 1996) with a model of troponin-myosin concentration (Yaniv et al., 2006), whose parameters were modified to fit atrial force data (Beyer et al., 1986; Komai and Rusy, 1990). The energetics model was a modified version of a model described by Cortassa et al. (Cortassa et al., 2006) and

included mitochondrial  $\text{Ca}^{2+}$  dynamics that was based on an earlier report (Nguyen et al., 2007). The interconnection between the models is described in Figure 1B. Our suggestion for the metabolic steps affected by the  $\text{Ca}^{2+}$  push and pull mechanisms are shown in the mitochondrion part of Figure 1A.

For conciseness, only novel assumptions and modifications in the model equations are described here, while the full model and the modified parameters is described in the supplement.

### 2.8.1 Assumptions

- (i) The ATP consumption by  $\text{Na}^+$ - $\text{K}^+$  ATPase and the membranal  $\text{Ca}^{2+}$  pump is low, thus we used the original equation described in (Lindblad et al., 1996).
- (ii) The force generation can be described by a four-state rather than a two-state kinetics (Yaniv et al., 2006) model.
- (iii) Similar to NADH,  $\text{FADH}_2$  concentration is not constant (Harris and Das, 1991).
- (iv) As the reducing reagents,  $\text{FADH}_2$  and NADH are created in the TCA cycle in a 1:4 ratio ( $\text{FADH}_2$ :NADH), and we assume that their consumption by the electron transfer chain follows the same ratio (Harris and Das, 1991).
- (v) Regulation of oxidative phosphorylation by the cellular energy demands can be modeled using a push and pull mechanism (Balaban, 2009).
- (vi)  $\text{Ca}^{2+}$  regulates the activity of  $\text{F}_1\text{F}_0$ -ATPase (Balaban, 2012).

### 2.8.2 Modification in the model

An ATP-dependent variable was added to the original uptake current of  $\text{Ca}^{2+}$  into the sarcoplasmic reticulum (SR) equation in (Lindblad et al., 1996):

$$I_{\text{up}} = I_{\text{up,max}} \cdot \frac{[\text{ATP}]_i}{7.977} \frac{\frac{[\text{Ca}^{2+}]_i}{K_{\text{cy,Ca}}} - \frac{K_{\text{cs}}^2 [\text{Ca}^{2+}]_{\text{up}}}{K_{\text{sr,Ca}}}}{\frac{[\text{Ca}^{2+}]_i + K_{\text{cy,Ca}}}{K_{\text{cy,Ca}}} + \frac{K_{\text{cs}} ([\text{Ca}^{2+}]_{\text{up}} + K_{\text{sr,Ca}})}{K_{\text{sr,Ca}}}} \quad (1)$$

where  $I_{\text{up,max}}$  is the maximal calcium uptake current into the SR,  $K_{\text{cy,Ca}}$  is the equilibrium binding  $\text{Ca}^{2+}$  concentration on the cytosolic side  $[[\text{Ca}^{2+}]_i]$ ,  $K_{\text{sr,Ca}}$  is the equilibrium binding  $\text{Ca}^{2+}$  concentration in the uptake compartment of the SR side,  $K_{\text{cs}}$  is a translocation constant and  $[\text{Ca}^{2+}]_{\text{up}}$  is the  $\text{Ca}^{2+}$  concentration in the uptake compartment of the SR.

Because the force is described by four state that are affected by  $\text{Ca}^{2+}$ , instead of on and off kinetics, the amount of bound  $\text{Ca}^{2+}$  to the tropomyosin is described by:

$$\frac{dO_{\text{TnCa}}}{dt} = F_{\text{kl}} [\text{Ca}^{2+}]_i (1 - A - \text{TT} - U) + F_{\text{kl}} [\text{Ca}^{2+}]_i U - \text{TT}K_{-1} - AK_{-1} \quad (2)$$

where  $K_{-1}$  describes the dependence of  $\text{Ca}^{2+}$  affinity on the number of strong cross-bridges and  $F_{\text{kl}}$  is the rate constant of calcium binding to low-affinity troponin sites.  $A$  is the density of regulatory units with bound  $\text{Ca}^{2+}$  and adjacent weak cross-bridges.  $\text{TT}$  is the density of regulatory units with bound  $\text{Ca}^{2+}$  and adjacent strong cross-bridge.  $U$  is the density of regulatory units without bound  $\text{Ca}^{2+}$  but with adjacent strong cross-bridges.

We modified the energetics equation in (Cortassa et al., 2006) to include regulation by mitochondrial  $\text{Ca}^{2+}$  ( $[\text{Ca}^{2+}]_{\text{m}}$ ), as suggested by (Harris and Das, 1991). Thus, the rate of pyruvate dehydrogenase can be described by:

$$V_{\text{PDH}} = k_{\text{PDH}} \cdot C_{\text{PYR}} \cdot \left( \frac{[\text{Ca}^{2+}]_{\text{m}}}{[\text{Ca}^{2+}]_{\text{m}} + k_{\text{CaAcCoA}}} \right) \quad (3)$$

where  $k_{\text{PDH}}$  is the catalytic constant of pyruvate dehydrogenase (PDH),  $C_{\text{PYR}}$  is the pyruvate concentration and  $k_{\text{CaAcCoA}}$  is the Michaelis constant representing the regulatory effect of  $\text{Ca}^{2+}$  on PDH.

The respiration-driven proton pump is based on (Cortassa et al., 2006), with the modification indicated below:

Mitochondrial  $\text{NAD}^+$  is assumed to be conserved according to the following relation:

$$[\text{NAD}] = C_{\text{PN}} - [\text{NADH}] \quad (4)$$

where  $C_{\text{PN}}$  is the total sum of mitochondrial pyridine nucleotides.

$$A_{\text{resNADH}} = \frac{RT}{F} \ln \left( K_{\text{res}} \sqrt{\frac{[\text{NADH}]}{[\text{NAD}]}} \right) \quad (5)$$

$$A_{\text{resFLV}} = \frac{RT}{F} \ln \left( K_{\text{res}} \sqrt{\frac{[\text{FADH}_2]}{[\text{FAD}]}} \right) \quad (6)$$

$$[\text{FAD}] = \text{Tot}_{\text{FAD}} - [\text{FADH}_2], \quad (7)$$

where  $K_{\text{res}}$  is the equilibrium constant of respiration,  $[\text{FADH}_2]$  is the concentration of reduced FAD,  $[\text{FADH}]$  is the concentration of oxidized FAD and  $\text{Tot}_{\text{FAD}}$  is the total concentration of  $\text{FADH}_2$  and FAD.

As the reducing reagents,  $\text{FADH}_2$  and  $\text{NADH}$  are created in the TCA cycle in a 1:4 ratio ( $\text{FADH}_2:\text{NADH}$ ) and we assume that their consumption by the electron transfer chain follows the same ratio. This means that 1/5 of oxygen consumption is attributed to  $\text{FADH}_2$ -fueled and 4/5 to  $\text{NADH}$ -fueled electron transfer cycles:

$$A_{\text{res}} = \frac{4}{5} A_{\text{res\_NADH}} + \frac{1}{5} A_{\text{res\_FLV}} \quad (8)$$

In a modification of the original formulation in (Cortassa et al., 2006), it is also considered that the complex II electrons are input by SUC through  $\text{FADH}_2$  to the respiratory chain:

$$A_{\text{res(F)}} = \frac{RT}{F} \ln \left( K_{\text{res(F)}} \sqrt{\frac{[\text{FADH}_2]}{[\text{FAD}]}} \right) \quad (9)$$

$$V_{\text{He(F)}} = 4 \rho^{\text{res(F)}} \frac{(r_a \exp(\frac{A_{\text{res(F)}} F}{RT}) - (r_a + r_b) \exp(\frac{86F\Delta\mu_{\text{H}}}{RT}))}{((1 + r_1 \exp(\frac{A_{\text{res(F)}} F}{RT})) \exp(\frac{56F\Delta\psi_{\text{e}}}{RT}) + (r_2 + r_3 \exp(\frac{A_{\text{res(F)}} F}{RT})) \exp(\frac{86F\Delta\mu_{\text{H}}}{RT})} \quad (10)$$

The flux of protons driven by  $\text{FADH}_2$  oxidation ( $V_{\text{He(F)}}$ ) has the same form as  $V_{\text{He}}$ , except for the adjustment of the redox potential and the  $\text{H}^+$  stoichiometry.  $\rho^{\text{res(F)}}$  is the concentration of electron carriers (respiratory complexes II-III-IV) and  $K_{\text{res(F)}}$  is the equilibrium constant of  $\text{FADH}_2$  oxidation.

The regulation of oxidative phosphorylation by the cellular energy demands is modeled using a push and pull mechanism. ADP activates enzymes in the Krebs cycle, which “pushes” the respiratory flux toward ATP generation (Harris and Das, 1991). In parallel, ADP controls ATP synthase by its availability, thereby “pulling” ATP production by increasing the respiratory flux (Chance and Williams, 1955):

$$\text{pull} = \frac{V_{\text{ATPase}}}{k_{\text{ATPase}}} \quad (11)$$

$$V_{\text{O}_2} = \rho^{\text{res}} \text{pull} \frac{((r_a + r_{c1} \exp(\frac{6FA\Delta\psi_{\text{e}}}{RT})) \exp(\frac{A_{\text{res}} F}{RT}) - r_a \exp(\frac{86F\Delta\mu_{\text{H}}}{RT}) + r_{c2} \exp(\frac{A_{\text{res}} F}{RT}) \exp(\frac{86F\Delta\mu_{\text{H}}}{RT}))}{((1 + r_1 \exp(\frac{A_{\text{res}} F}{RT})) \exp(\frac{6FA\Delta\psi_{\text{e}}}{RT}) + (r_2 + r_3 \exp(\frac{A_{\text{res}} F}{RT})) \exp(\frac{86F\Delta\mu_{\text{H}}}{RT}))} \quad (12)$$

where  $r_{c1}$  and  $r_{c2}$  are the sum of products of rate constants, and  $k_{\text{ATPase}}$  is defined as the coupling coefficient representing the pull effect of the ATP synthase on the activity of the electron transfer chain.

According to the concept of respiratory control, mitochondrial function is governed by the availability of ADP and  $\text{P}_i$ . The chemiosmotic hypothesis dictates that  $\Delta\psi_{\text{m}}$  is lowered by an  $\text{H}^+$  influx, which drives the production of ATP by  $\text{F}_1\text{F}_0$ -ATPase.

$$V_{\text{ATPase}} = -30 \cdot \rho^{\text{F}_1} \frac{((10^2 p_a + p_{c1} \exp(\frac{3FA\Delta\psi_{\text{e}}}{RT})) \exp(\frac{FA_{\text{F}_1}}{RT}) - (p_a \exp(\frac{3FA_{\text{H}_2}}{RT}) + p_{c2} \exp(\frac{FA_{\text{F}_1}}{RT}) \exp(\frac{3FA\Delta\psi_{\text{e}}}{RT})))}{((1 + p_1 \exp(\frac{FA_{\text{F}_1}}{RT})) \exp(\frac{3FA\Delta\psi_{\text{e}}}{RT}) + (p_2 + p_3 \exp(\frac{FA_{\text{F}_1}}{RT})) \exp(\frac{3FA\Delta\mu_{\text{H}}}{RT}))} \cdot (1 - \exp(-\frac{C_{\text{a}_m}}{K_{\text{CaATP}}})) \quad (13)$$

$$V_{\text{H}_2\text{O}} = -3 \rho^{\text{F}_1} \frac{(10^2 p_a (1 + \exp(\frac{FA_{\text{F}_1}}{RT})) - (p_a + p_b) \exp(\frac{3FA_{\text{H}_2}}{RT}))}{((1 + p_1 \exp(\frac{FA_{\text{F}_1}}{RT})) \exp(\frac{3FA\Delta\psi_{\text{e}}}{RT}) + (p_2 + p_3 \exp(\frac{FA_{\text{F}_1}}{RT})) \exp(\frac{3FA\Delta\mu_{\text{H}}}{RT}))} \quad (14)$$

$$A_{\text{F}_1} = \frac{RT}{F} \ln \left( K_{\text{F}_1} \frac{[\text{ATP}]_{\text{m}}}{[\text{ADP}]_{\text{m}} [\text{P}_i]} \right) \quad (15)$$

$$[\text{ATP}]_{\text{m}} = C_{\text{A}} - [\text{ADP}]_{\text{m}} \quad (16)$$

where  $p_a$ ,  $p_b$ ,  $p_{c1}$ ,  $p_{c2}$ ,  $p_1$ ,  $p_2$  and  $p_3$  are the sum of products of rate constants,  $\rho^{\text{F}_1}$  is the  $\text{F}_1\text{F}_0$ -ATPase concentration,  $K_{\text{F}_1}$  is the equilibrium

constant of ATP hydrolysis,  $P_i$  is the inorganic phosphate concentration and  $C_A$  is the total sum of mitochondrial adenine nucleotides.

Experimental data (see results section) of  $Ca^{2+}$  transients, oxygen consumption and flavoprotein at a 1 Hz stimulus frequency were used as input for the computational model, and the values predicted at 2 Hz and 3 Hz stimulus frequencies were compared to the experimental results.

### 2.8.3 Modeling the “push” and “pull” mechanisms

To eliminate the “pull” mechanism, the effect of  $Ca^{2+}$  on ATP synthase was withheld by fixing the mitochondrial  $Ca^{2+}$  to its initial condition in the  $V_{ATPase}$  equation, so only the ADP “pull” played a role. To shut down the “push” mechanism, the mitochondrial  $Ca^{2+}$  was fixed at a constant value (its initial condition) throughout the model, which canceled the  $Ca^{2+}$  “push” effect on the TCA cycle and ATP synthase. In addition, the coupling variable between ATP synthase activity and the electron transfer chain oxygen consumption was fixed to its initial value, which eliminated “pull” entirely.

### 2.8.4 ATP consumption

ATP consumption was calculated as the sum of the three main energy-consuming processes in the cell: active membrane transporters,  $Ca^{2+}$  intake by the SR and sarcomere contractile elements. For the membrane component, the  $Na^+K^+$  ATPase and the membrane  $Ca^{2+}$  pump were considered:

$$\left. \frac{d[ATP]}{dt} \right|_{membranal} = \frac{(I_{NaK} + I_{Cap})A_{cap}}{V_{myo}F} \quad (17)$$

where  $I_{NaK}$  and  $I_{Cap}$  are the currents per unit area,  $A_{cap}$  is the capacitive cell surface area,  $V_{myo}$  is the myocyte volume and  $F$  is the Faraday constant.

ATP consumption by the SR is correlative to  $Ca^{2+}$  uptake by the SR:

$$\left. \frac{d[ATP]}{dt} \right|_{SR} = \frac{0.5I_{up}}{V_{myo}F} \quad (18)$$

where  $I_{up}$  is the SR uptake current,  $V_{myo}$  is the myocyte volume and  $F$  is the Faraday constant. The current is multiplied by 0.5 to account for the stoichiometry of the calcium pump reaction.

The sarcomere energy consumption is calculated as part of the sarcomere model, in Eq. 112 in the supplement:

$$\left. \frac{d[ATP]}{dt} \right|_{sarcomere} = V_{AM} \quad (19)$$

The total energy consumption is the sum of the three:

$$\frac{d[ATP]}{dt} = \left. \frac{d[ATP]}{dt} \right|_{membranal} + \left. \frac{d[ATP]}{dt} \right|_{SR} + \left. \frac{d[ATP]}{dt} \right|_{sarcomere} \quad (20)$$

## 2.9 Numerical methods

The software was run in MATLAB (The MathWorks, Inc., Natick, MA, United States). Numerical integration was performed using the MATLAB ode23tb stiff solver. Impulse stimulations were modeled as boundary conditions and the ODE was solved on the intervals between impulses. A 1-s quiescent

window was added between stimulation rates to ensure the completion of the last beat before initiation of a new one. Computations were performed on an Intel(R) Core(TM) i7-8550U CPU @ 1.80 GHz machine with 16 GB RAM. Upon publication, the source code of the numerical model will be available at <http://bioelectric-bioenergetic-lab.net.technion.ac.il> and on <https://github.com/yyLabPhysAI/energetics-atrium>.

## 3 Results

### 3.1 Increase in electrical stimulus frequency increases ATP supply and demand

Fundamental experiments were first performed to verify that an increase in electrical stimulus frequency increases ATP supply. In a fully coupled system, oxygen consumption is an indicator of ATP production, i.e., supply. Increases in stimulus frequency increased oxygen consumption and were statistically significant at 3 Hz compared to 1 Hz (Figure 2). Only the values of oxygen consumption at 1 Hz stimulus frequency were used as input to the computational model, and the predicted model values at 2 and 3 Hz stimulus frequency were compared to the experimental results (see below).

Using the computational model, we found that at 1 Hz stimulus frequency (Figure 3A), the SERCA pump (56.9%) and the myofilaments (43%) were the major ATP consumers, while maintenance of the membrane homeostasis (sodium-potassium pump and  $Ca^{2+}$  pump) consumed only 0.05% of the ATP budget. By calculating the relative consumption of ATP by the above consumers we found that increasing the stimulus frequency to 2 Hz and 3 Hz increased the ATP consumption rate by the SERCA and sarcomeres, due to an increased uptake rate (Figure 3B, from 3.48 pA at 1 Hz to 3.81 pA and 4.3 pA at 2 Hz and 3 Hz, respectively), and in the case of force, increased average systolic force (Figure 3C, from  $3.31 \cdot 10^5 \frac{\mu N}{mm^2}$  at 1 Hz to  $3.34 \cdot 10^5 \frac{\mu N}{mm^2}$  and  $3.53 \cdot 10^5 \frac{\mu N}{mm^2}$  at 2 and 3 Hz, respectively). Supplementary Figure S1 shows the ionic currents and pumps measured in response to increasing electrical stimulus rates. The model predicted that the increase in ATP demand was mainly due to an increase in the rate, and not amplitude, of the currents because the amplitude of the sodium-potassium pump and  $Ca^{2+}$  pump currents slightly decreased with increased stimulus frequency. On change of the stimulus frequency (2 Hz and 3 Hz), there was no change in the relative ATP consumption by the consumers compared to 1 Hz. Thus, the rate-dependent changes in contractility and  $Ca^{2+}$  handling are the same, likely because the majority of  $Ca^{2+}$  is bound to troponin.

### 3.2 $Ca^{2+}$ is an important regulator of ATP supply-to-demand matching

Our hypothesis was that  $Ca^{2+}$  (Figure 3D) is a key regulator of ATP supply-to-demand matching in the atrium. Thus, we experimentally measured its kinetic under different electrical stimulation rates. We found that at 1 Hz, the  $t_{50}$  (50% decline time of the  $Ca^{2+}$  signal from the peak) was  $166.8 \pm 168$  ms and  $t_{90}$  (90% decline time of the  $Ca^{2+}$  signal from the peak) was  $407 \pm$

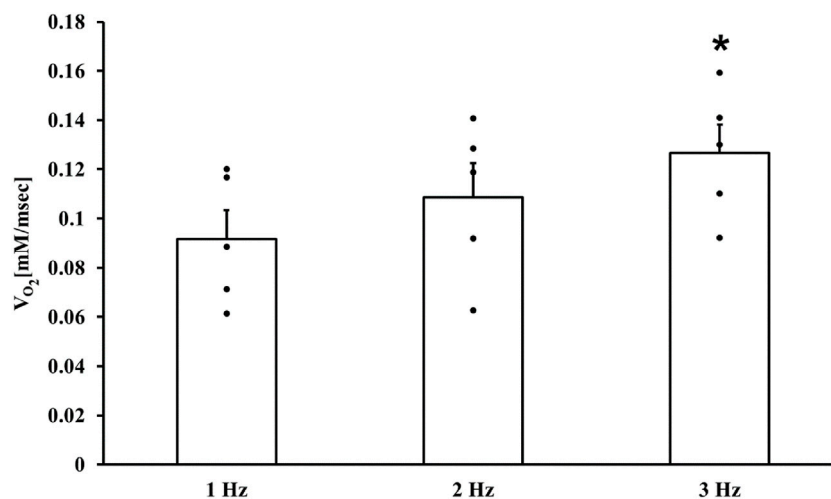


FIGURE 2

ATP supply in atrial cells. Respiration rates of isolated atrial cell suspensions ( $n = 5$ ) electrically stimulated at 1, 2 and 3 Hz  $*p < 0.05$  vs. 1 Hz.

204 ms ( $n = 36$  cells). At 3 Hz,  $t_{50}$  was  $115 \pm 48$  ms and  $t_{90}$  was  $187 \pm 48$  ms,  $n = 36$  (Figure 3E). We then fitted the parameters of the model, including channel and transporter dynamics and conductance, enzyme kinetics and initial values of state variables, to achieve similar  $Ca^{2+}$  kinetics at a 1 Hz stimulus frequency. The parameters were selected to fulfill additional criteria, which included ensuring model non-divergence, TCA cycle stability, and maintaining all state variables within physiological ranges. At 1 Hz stimulus frequency, the model predicted a  $t_{50}$  of 145.2 ms and  $t_{90}$  of 423.2 ms, which were both in the range of the experimental values (Figure 3E). We compared the model predictions to the experimental measurements at 3 Hz. At 3 Hz stimulus frequency, the model predicted a  $t_{50}$  of 110.2 ms and  $t_{90}$  of 247.1 ms, which aligned with the experimental results. Note that small differences in  $t_{90}$  may be related to frequency-dependent influx and outflux kinetics of  $Ca^{2+}$  from the SR.

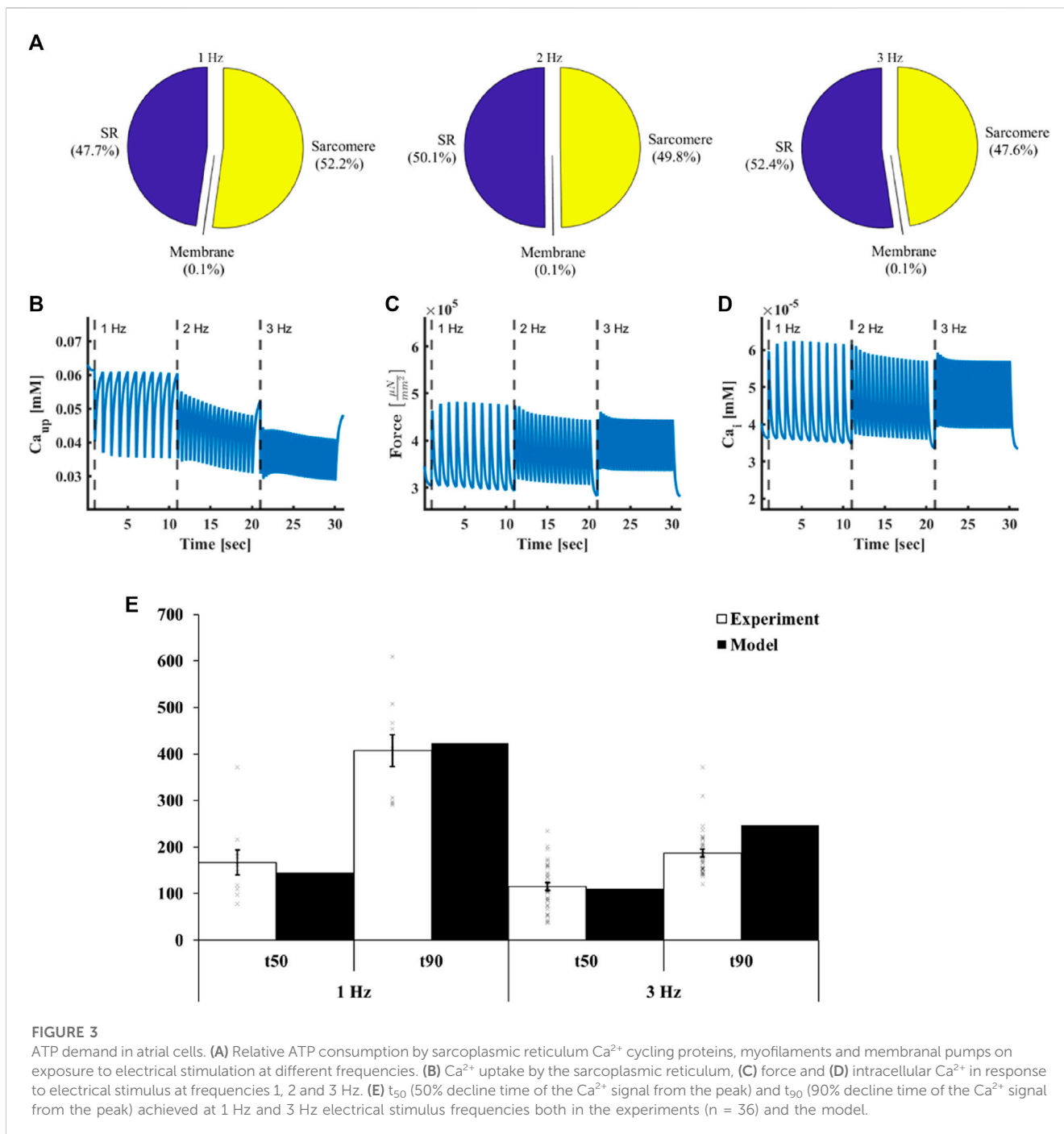
In the computational model, the increase in intracellular  $Ca^{2+}$  in response to an increase in stimulus frequency led to an accumulation of mitochondrial  $Ca^{2+}$  (Figure 4A, from  $2.42 \cdot 10^{-5}$  mM at 1 Hz to  $2.63 \cdot 10^{-5}$  mM and  $2.81 \cdot 10^{-5}$  mM at 2 and 3 Hz, respectively). With increased stimulation rates, metabolic homeostasis, quantified by  $FADH_2$  (Figure 4B, from 5.41 mM at 1 Hz to 5.41 mM and 5.42 mM at 2 and 3 Hz, respectively) or NADH (Figure 4C, from 5.42 mM at 1 Hz to 5.43 mM and 5.44 mM at 2 and 3 Hz, respectively) concentration, was maintained, while oxygen consumption increased (Figure 4D, from  $0.104 \frac{mM}{ms}$  at 1 Hz to  $0.109 \frac{mM}{ms}$  and  $0.113 \frac{mM}{ms}$  at 2 and 3 Hz, respectively) in a fashion similar to that measured experimentally (Figure 2).  $FADH_2$  levels remained constant upon increase of stimulus frequency from 1 Hz to 3 Hz, in accordance with previous experimental results (Kirschner Peretz et al., 2017) (Figure 4E). Similarly, the computational model predicted that metabolic homeostasis of all Krebs cycle metabolites was maintained (Figure 5). Note that although metabolic homeostasis existed in steady state, effects of  $Ca^{2+}$  oscillation on alpha ketoglutarate, succinyl-CoA and succinate were observed (Figures 5D–F). Yet, the oscillation amplitude was below the experimental detection level.

### 3.3 $Ca^{2+}$ regulates ATP supply via both push and pull modes

Next, we explored the regulation of ATP synthesis by  $Ca^{2+}$ . Both push (mitochondrial  $Ca^{2+}$  activates metabolite flux and enzymes in the Krebs cycle) and pull (mitochondrial  $Ca^{2+}$  activates ATP synthase) mechanisms were suggested (Harris and Das, 1991). Figure 6 shows the simulated oxygen consumption (Figure 6A),  $FADH_2$  concentration (Figure 6B), intracellular (Figure 6C) and mitochondrial (Figure 6D) ATP levels in response to increasing stimulus frequencies. When both  $Ca^{2+}$  push and pull mechanisms were intact, oxygen consumption increased (from  $0.104 \frac{mM}{ms}$  at 1 Hz to  $0.109 \frac{mM}{ms}$  and  $0.113 \frac{mM}{ms}$  at 2 Hz and 3 Hz, respectively) in response to increased stimulus frequency, matching the experimental results, while metabolic homeostasis was maintained, as described elsewhere (Kirschner Peretz et al., 2017) and shown here (Figure 4E). However, when the ATP synthase pull mechanism was disabled prior to increased stimulus frequency, oxygen consumption did not change after reaching steady state (from  $0.096 \frac{mM}{ms}$  at 1 Hz to  $0.101 \frac{mM}{ms}$  and  $0.103 \frac{mM}{ms}$  at 2 and 3 Hz, respectively), excluding a transient effect at the beginning of the simulation, in contrast to experimental results. When both push and pull mechanisms were eliminated, no change in oxygen consumption was obtained (from  $0.091 \frac{mM}{ms}$  at 1 Hz to  $0.091 \frac{mM}{ms}$  and  $0.091 \frac{mM}{ms}$  at 2 Hz and 3 Hz, respectively), while mitochondrial ATP concentrations decreased and cellular ATP remained constant. Thus, in our simulation, the push mechanism was necessary to maintain metabolic homeostasis.

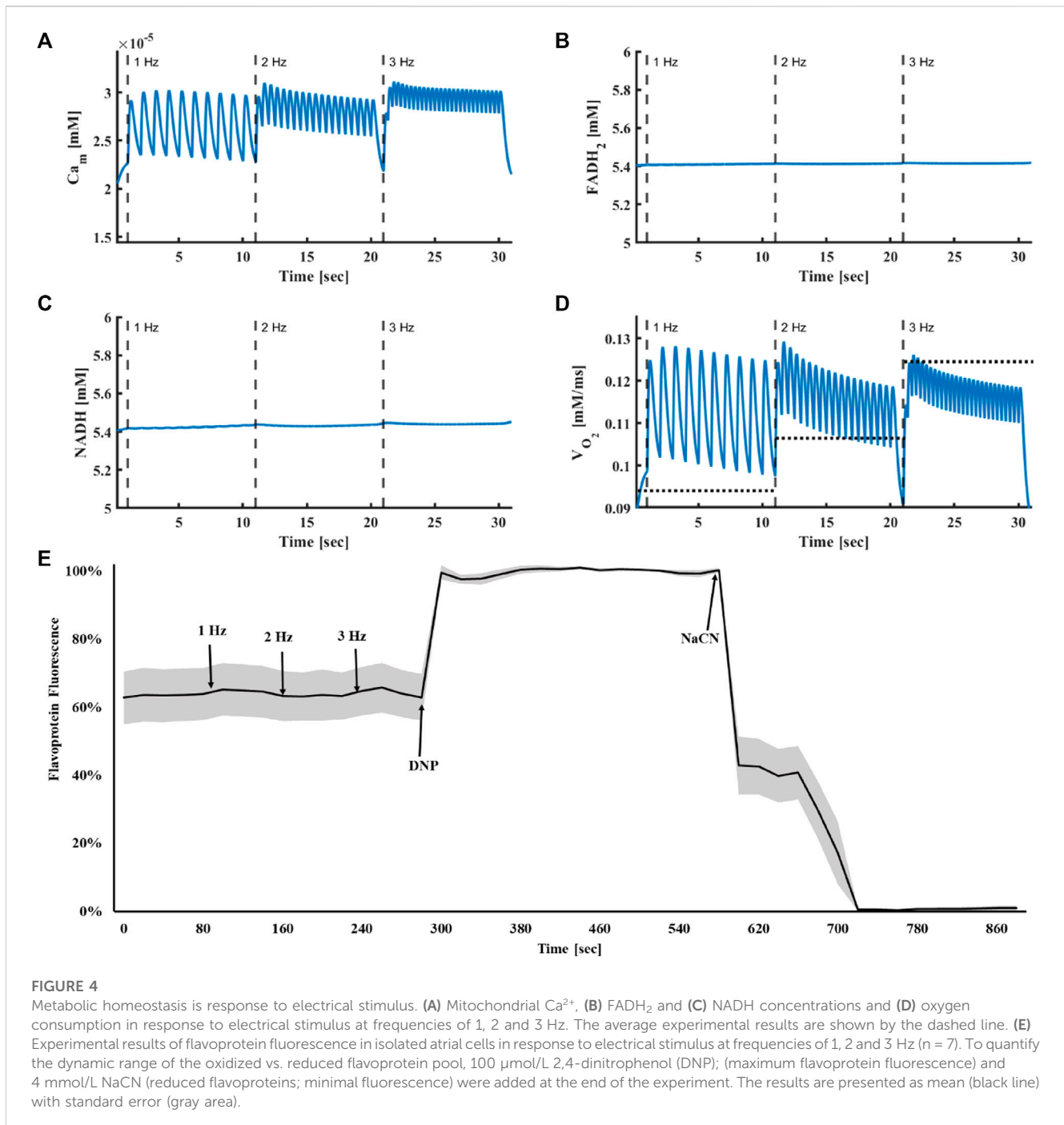
### 3.4 Metabolic homeostasis is maintained in response to change in stimulus frequency

Previous works have used computational models to demonstrate the existence of “push” and “pull” mechanisms in ventricular cells,



which explain the time-dependent behavior of NADH (Cortassa et al., 2006). Others have measured the time-dependent behavior of NADH in ventricular rat trabeculae using a protocol in which the stimulus frequency was increased from 0.25 Hz to 2 Hz and then returned to 0.25 Hz (Brandes and Bers, 1999; 2002). We reproduced these experiment with a similar protocol in rabbit atrial cells. (Figure 7). When the frequency was increased from 0.25 Hz to 2 Hz ( $96.8\% \pm 5.6\%$ ) or when stimulus frequency was returned to 0.25 Hz after 2 Hz stimulation ( $95.2\% \pm 4.2$ ) ( $n = 5$  cells), no measurable frequency-dependent change was observed in flavoprotein fluorescence (a reciprocal proxy of NAD).

Our computational results showed that when the stimulus frequency was rapidly raised from 0.25 Hz to 2 Hz and then returned to 0.25 Hz, mitochondrial  $\text{Ca}^{2+}$  (Figure 8A from  $2.38 \cdot 10^{-5} \text{mM}$  at 0.25 Hz to  $2.67 \cdot 10^{-5} \text{mM}$  at 2 Hz), oxygen consumption (Figure 8D, from  $0.105 \frac{\text{mM}}{\text{ms}}$  at 0.25 Hz to  $0.113 \frac{\text{mM}}{\text{ms}}$  at 2 Hz) increased and decreased, respectively, but  $\text{FADH}_2$  (Figure 8C, from  $5.414 \text{mM}$  at 0.25 Hz to  $5.417 \text{mM}$  at 2 Hz) and NADH (Figure 8D, from  $5.443 \text{mM}$  at 0.25 Hz to  $5.446 \text{mM}$  at 2 Hz) levels were maintained. Note, that at the 2 Hz stimulation rate, a negative staircase of diastolic  $\text{Ca}^{2+}$  was observed. This phenomenon was likely due to changes in the



kinetics of  $\text{Ca}^{2+}$  uptake and release from the SR. This phenomenon was consistent in all  $\text{Ca}^{2+}$  compartments. Nevertheless, the behavior of  $\text{Ca}^{2+}$  on all components across frequencies was as expected; higher frequencies elevated the mean cytoplasmic and mitochondrial  $\text{Ca}^{2+}$  concentrations, creating a higher contraction force in the sarcomeres, which signaled the mitochondria that energy consumption increased.

To confirm that  $\text{Ca}^{2+}$  plays a vital role in maintaining metabolic homeostasis during rapid increases in ATP demand, we disabled  $\text{Ca}^{2+}$  activation in either the push or pull pathways. With the pull mechanism disabled, no change in oxygen consumption occurred (from  $0.096 \frac{\text{mM}}{\text{ms}}$  at

$0.25 \text{ Hz}$  to  $0.102 \frac{\text{mM}}{\text{ms}}$  at  $2 \text{ Hz}$ ), but metabolic homeostasis existed. However, when  $\text{Ca}^{2+}$  was absent from both the “pull” and “push” pathways, metabolic homeostasis was disrupted.

## 4 Discussion

In the present study, we investigated the role of  $\text{Ca}^{2+}$  in ATP supply-to-demand matching in atrial cells. We presented here, for the first time, a computational model that included both the main ATP consumers, mitochondrial bioenergetics and their regulators in

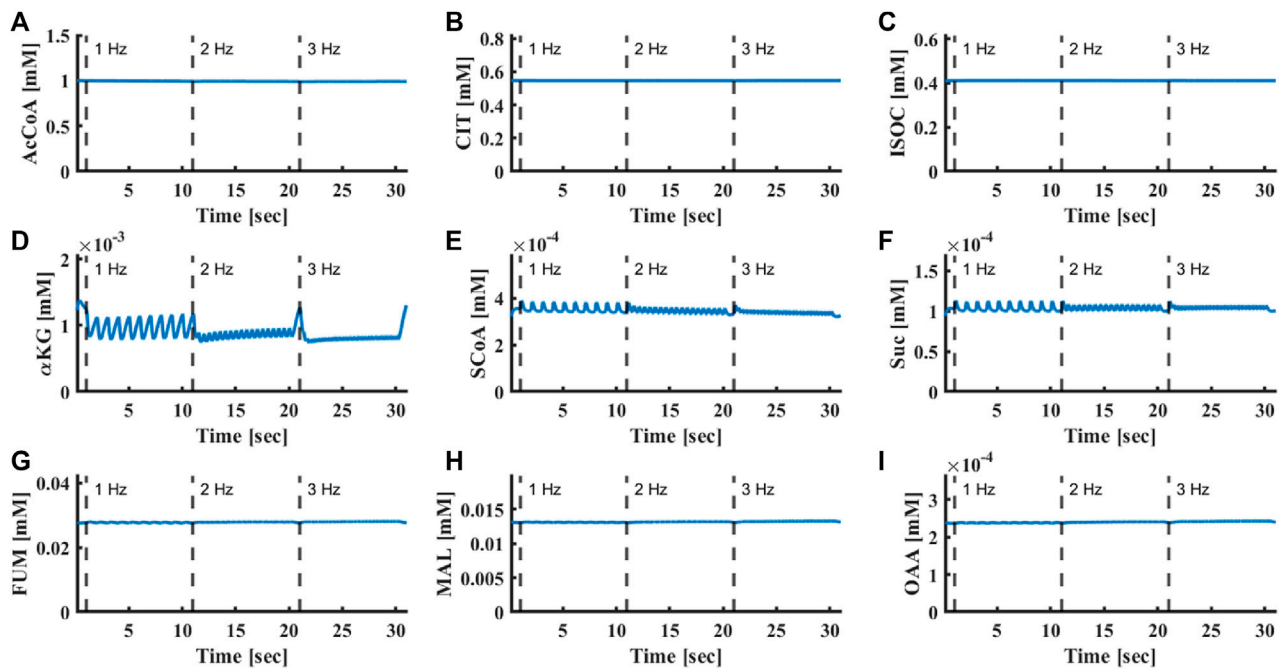


FIGURE 5

Oscillation of Krebs cycle protein concentrations. (A) Acetyl-CoA, (B) citrate, (C) isocitrate, (D)  $\alpha$ -ketoglutarate, (E) succinyl-CoA, (F) succinate, (G) fumarate, (H) L-malate and (I) oxaloacetate concentrations in response to electrical stimulus at frequencies of 1, 2 and 3 Hz.

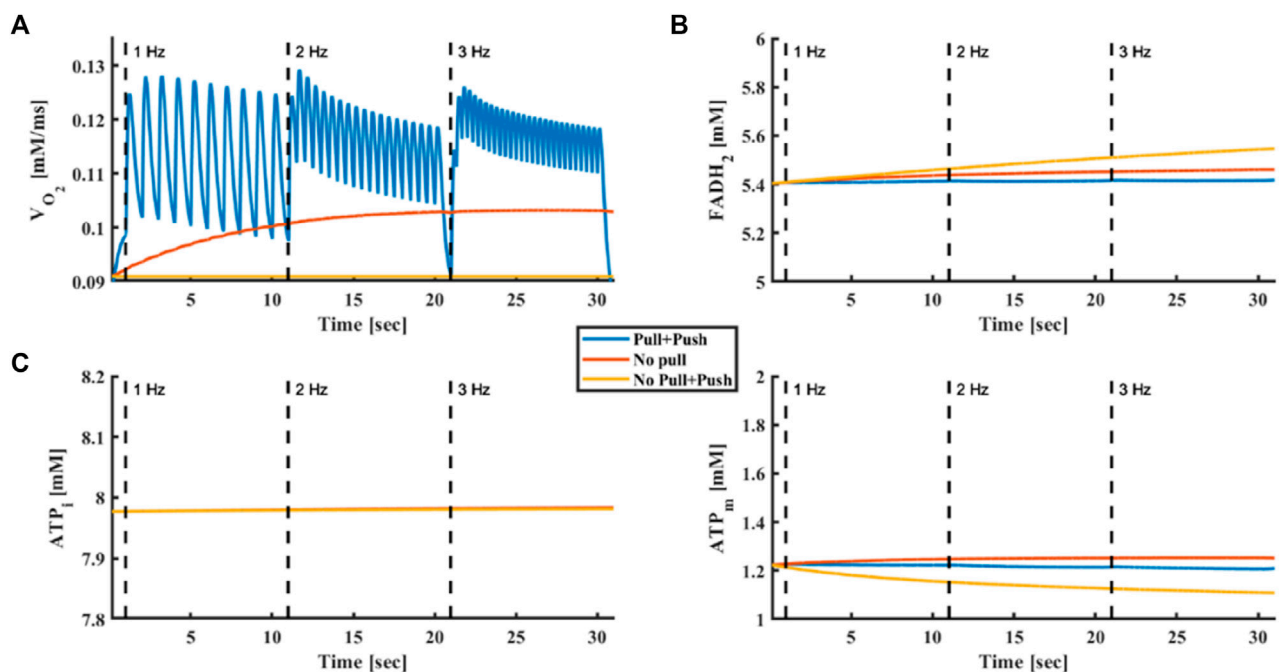


FIGURE 6

Push and pull mechanisms driven by  $\text{Ca}^{2+}$ . (A) Oxygen consumption, (B)  $\text{FADH}_2$  concentration, (C) intracellular ATP and (D) mitochondrial ATP in response to electrical stimulus at frequencies of 1, 2 and 3 Hz. The model was tested without push and pull mechanisms driven by  $\text{Ca}^{2+}$ , with only a  $\text{Ca}^{2+}$  push mechanism and with both push and pull mechanisms driven by  $\text{Ca}^{2+}$ .

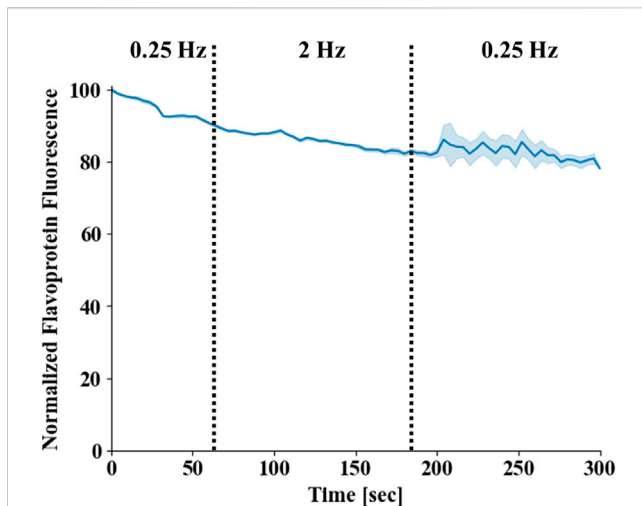


FIGURE 7

Flavoprotein homeostasis in atrial cells. Flavoprotein fluorescence in isolated atrial cells. The stimulus frequency was raised from 0.25 Hz to 2 Hz and then returned to 0.25 Hz ( $n = 4$ ). Mean fluorescence is presented by a blue line and standard error by the light blue area around it. Note that the standard error increased towards the end of protocol, as the measurement of two of the cells was terminated before the end of the protocol due to technical issues.

atrial cells. The model predicted that increases in the electrical stimulation frequency increase ATP demand and mitochondrial  $\text{Ca}^{2+}$  in parallel to increased oxygen consumption. Clamping of mitochondrial  $\text{Ca}^{2+}$  resulted in the elimination of the coupling between stimulation rate and oxygen consumption, supporting

the first hypothesis that  $\text{Ca}^{2+}$  is an important regulator of ATP supply-to-demand matching. In contrast to the experimental results, the model predicted that on elimination of the role of  $\text{Ca}^{2+}$  as a “pull” modulator, oxygen consumption does not increase in response to electrical stimulation, supporting the second hypothesis that  $\text{Ca}^{2+}$  acts both in “pull” and “push” modules. Finally, both experimental evidence and model predictions showed no rapid time-dependent changes in mitochondrial flavoprotein fluorescence in response to abrupt or slow changes in workload, supporting the third hypothesis that metabolic homeostasis is maintained in atrial cells in response to abrupt or slow increases in workload.

Our model predicted that  $\text{Ca}^{2+}$  is a key regulator of ATP supply-to-demand matching. At an increased workload, changes in mitochondrial  $\text{Ca}^{2+}$  were causally correlated with changes in oxygen consumption, while the other metabolites remained constant (i.e., showed no correlation with oxygen consumption). The comparison was enabled by novel oxygen consumption measurements, performed for the first time in isolated and electrically stimulated atrial cells.  $\text{Ca}^{2+}$  was regulated by both ATP supply and by the mitochondria that produce ATP. We simulated the two main ATP-consuming processes, both of which are  $\text{Ca}^{2+}$ -dependent, i.e., pumping  $\text{Ca}^{2+}$  by the SERCA and force generation by myofilaments, to which the majority of  $\text{Ca}^{2+}$  is attached (Bers, 2002).  $\text{Ca}^{2+}$  enters the mitochondria through the mitochondrial  $\text{Ca}^{2+}$  uniporter (Baughman et al., 2011; De Stefani et al., 2011) and activates energy-related mechanisms, and is extruded by the mitochondrial  $\text{Na}^+$ - $\text{Ca}^{2+}$  exchanger (Palty et al., 2010). Eliminating the  $\text{Ca}^{2+}$  effect on ATP synthase (“pull” effect) diminished the correlation between mitochondrial  $\text{Ca}^{2+}$  and oxygen consumption. Moreover, without  $\text{Ca}^{2+}$  signaling, the metabolic homeostasis that we observed experimentally could not be maintained in the simulation. Thus, our

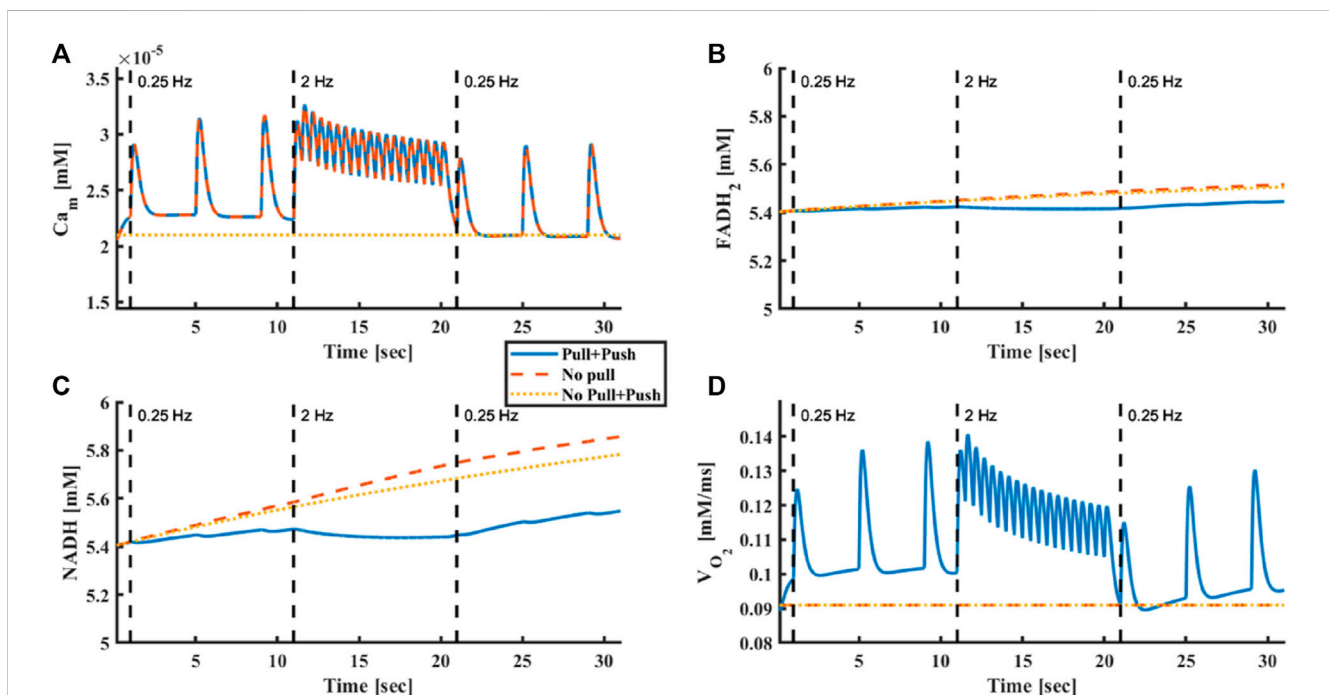


FIGURE 8

Model prediction of metabolic homeostasis in response to electrical stimulus. (A) Mitochondrial  $\text{Ca}^{2+}$ , (B)  $\text{FADH}_2$  concentration, (C) NADH concentration and (D) oxygen consumption in response to electrical stimulus frequency that was raised from 0.25 Hz to 2 Hz and then returned to 0.25 Hz. The model was tested without  $\text{Ca}^{2+}$  push and pull mechanisms, with only  $\text{Ca}^{2+}$  push mechanism and with both  $\text{Ca}^{2+}$  push and pull mechanisms.

results and simulation indicate that within the simulated workload range,  $\text{Ca}^{2+}$  is an important regulator of ATP supply to demand in both “push” and “pull” modes in atrial cells, as has been previously shown in ventricular cells (Cortassa et al., 2006; Bertero and Maack, 2018) and in isolated cardiac mitochondria (Baniene and Mildažienė, 2005). Note that when both the “push” and “pull” effects of  $\text{Ca}^{2+}$  were eliminated, ATP levels in the cytosol were still maintained in response to increases in workload, because presumably small changes in mitochondrial ADP pull the ATP synthase to increase ATP production. Thus, ADP is also an energy regulator in atrial cells.

It was postulated that “push” and “pull” modules lead to temporal changes in NADH levels in response to changes in workload (Cortassa et al., 2006). The differences in the relative response times of these two processes account for the transient overshoot and undershoot behavior of mitochondrial NADH documented in ventricular trabeculae (Brandes and Bers, 2002). However, in the current work, while  $\text{Ca}^{2+}$  “push” and “pull” effects were demonstrated in atrial cells, no transient overshoot or undershoot behavior was measured in response to change in overload. It is possible that different control mechanisms exist in atrial cells compared to the ventricle. Moreover, the experiments in ventricular trabeculae (Brandes and Bers, 2002) were performed at 22 °C, while the current work was conducted at 36 °C, which can result in different kinetics. Furthermore, it has been suggested that “push” is a  $\text{Ca}^{2+}$ -dependent mechanism while “pull” is only an ATP-related and not  $\text{Ca}^{2+}$ -dependent mechanism (Cortassa et al., 2006). It should be noted that Balaban and co-workers did not observe NADH transients in response to increased workload in the intact heart (Balaban, 2002) or in isolated mitochondria (Territo et al., 2001). Both here and in the isolated heart, the maintained metabolic homeostasis can be explained by the rapid increase in energy supply to meet energetic demands, triggered by fast parallel activation of the respiratory chain and Krebs cycle dehydrogenases by a cytoplasmic messenger, postulated here to be  $\text{Ca}^{2+}$ . Note that based on the model, the changes in mitochondrial  $\text{Ca}^{2+}$  led to small changes (less than 2%) in the rate of tangible  $\text{Ca}^{2+}$ -dependent effects on the Krebs cycle.

Our model faithfully reproduced experimental results. The model which was fitted on  $\text{Ca}^{2+}$  data measured under a 1 Hz stimulation rate, reproduced  $\text{Ca}^{2+}$  kinetics and oxygen consumption under a 3 Hz stimulation rate. The model also reproduced  $\text{FADH}_2$  homeostasis and predicted that metabolic homeostasis existed at all levels of bioenergetics, from the Krebs cycle enzymes to respiratory fluxes (Supplementary Figure S1). Note that all of our experiments were performed on rabbit cells, which exhibit excitation-contraction coupling mechanisms more similar to those of humans than mice, rats or guinea pigs (Bers, 2002). Although there are several promising computational models linking electrophysiology, ion homeostasis,  $\text{Ca}^{2+}$  handling, ATP consumption and mitochondrial energetics (Matsuoka et al., 2004; Cortassa et al., 2006; Yaniv et al., 2008), none of the models have been adjusted to atrial cells.

The model was developed to only consider supply-to-demand matching mechanisms working in a short window. It was shown before that several control mechanisms may work on a longer range (tens of seconds to minutes), such as CaMKII signaling (Yang et al., 2018) and the accumulation of intracellular sodium, which drive changes in  $\text{Ca}^{2+}$  handling via the sodium-calcium exchanger (Verkhatsky et al., 2018). Of note, even for short periods, there timing of activation of different mechanisms can differ;  $\text{Ca}^{2+}$  works on a beat-to-beat basis and was shown before to react faster than ADP to changes in demand (Cortassa et al., 2006).

## 5 Clinical insights

While a tight link between atrial fibrillation (AF) and electrophysiological and structural remodeling of the atria has been described (Voigt et al., 2014), recent evidence suggests that perturbations in energetic metabolites, which are tightly coupled with ion channel function and energy production, may be associated with transient or permanent AF. Alterations in  $\text{Ca}^{2+}$  handling have been correlated with AF (Dobrev and Nattel, 2008; Dobrev et al., 2011; Mason et al., 2020) and can lead to ATP supply-to-demand mismatch. Future experiments will be needed to retrain our model to provide predictions under AF conditions.

## 6 Limitations

The present model demonstrated the feasibility of mediation of energy supply-to-demand matching via  $\text{Ca}^{2+}$  and ADP in both “push” and “pull” modes. However, this work did not rule-out the possibility that other mechanisms and/or mediators are involved, such as posttranslational modification signaling, like PKA (Covian and Balaban, 2012). Additional experimental data on these signaling pathways will enable assessment of their relative role in ATP supply-to-demand matching.

Although cytosolic  $\text{Ca}^{2+}$  was measured in atrial cells, mitochondrial  $\text{Ca}^{2+}$  kinetics was not quantified. Such data are lacking due to the challenges of measurement of  $\text{Ca}^{2+}$  kinetics under high electrical stimulation frequencies. New methods are needed to complete this task.

The present work assumes that creatine kinase (CK) concentration is constant and does not model the CK kinetics in two compartments as was done in (Cortassa et al., 2006). In mice, near-total knockout of mitochondrial and/or cytosolic CK isoforms had a modest but measurable effect on cardiac performance measurements under normal as well as increased-demand conditions (Lygate et al., 2009; Lygate et al., 2013). Thus, under normal conditions the role of CK in ATP production is negligible. Future experiments will be necessary to understand the importance of the CK shuttle in ATP supply-to-demand matching in the atria.

Our computational model represented only the control mechanisms that operate on a time scale of seconds. Electrical stimulation for several minutes may activate additional energy balance maintenance mechanisms. Of note, even for longer periods of electrical stimulation (1 minute) metabolic homeostasis was maintained experimentally (Kirschner Peretz et al., 2017).

One should also take into consideration that some control mechanisms, such as  $\text{Ca}^{2+}$ , work on a beat-to-beat basis. However, the tools we used to quantify bioenergetics do not support such a level of resolution.

## 7 Conclusion

This work measured oxygen consumption and metabolic balance indicators in rabbit atrial cells and developed an integrated model of the electrophysiology, excitation-contraction coupling and mitochondrial bioenergetics of atrial cells. The model

reproduced the increase in oxygen consumption in response to electrical stimulation and maintained metabolic homeostasis under abrupt changes in workload. The model predicted that  $\text{Ca}^{2+}$  is an important regulator of ATP supply-to-demand matching and that  $\text{Ca}^{2+}$  works in both “push” and “pull” directions.

## Data availability statement

The original contributions presented in the study are included in the article/[Supplementary Material](#), further inquiries can be directed to the corresponding author.

## Ethics statement

The animal study was reviewed and approved by the Animal Care and Use Committee of the Technion (Ethics numbers: IL-118-10-13 and IL-001-01-19).

## Author contributions

YY designed the research, NK and NP performed the research, NK and NP analyzed the data, YY wrote the manuscript. YY, NK, and NP reviewed the manuscript and agreed to its final form. All authors contributed to the article and approved the submitted version.

## References

- Aslanidi, O. V., Boyett, M. R., Dobrzynski, H., Li, J., and Zhang, H. (2009). Mechanisms of transition from normal to reentrant electrical activity in a model of rabbit atrial tissue: Interaction of tissue heterogeneity and anisotropy. *Biophys. J.* 96, 798–817. doi:10.1016/j.bpj.2008.09.057
- Balaban, R. S. (2002). Cardiac energy metabolism homeostasis: Role of cytosolic calcium. *J. Mol. Cell. Cardiol.* 34, 1259–1271. doi:10.1006/JMCC.2002.2082
- Balaban, R. S. (2012). Perspectives on: SGP symposium on mitochondrial physiology and medicine: Metabolic homeostasis of the heart. *J. Gen. Physiol.* 139, 407–414. doi:10.1085/JGP.201210783
- Balaban, R. S. (2009). The role of  $\text{Ca}^{2+}$  signaling in the coordination of mitochondrial ATP production with cardiac work. *Biochim. Biophys. Acta - Bioenerg.* 1787, 1334–1341. doi:10.1016/j.bbabi.2009.05.011
- Baniēnē, R., and Mildažienē, V. (2005). Stimulation of ATP synthase by  $\text{Ca}^{2+}$  in heart mitochondria. *Biologija* 51 (1).
- Baughman, J. M., Perocchi, F., Girgis, H. S., Plovanich, M., Belcher-Timme, C. A., Sancak, Y., et al. (2011). Integrative genomics identifies MCU as an essential component of the mitochondrial calcium uniporter. *Nature* 476, 341–345. doi:10.1038/NATURE10234
- Bers, D. M. (2002). Cardiac excitation-contraction coupling. *Nature* 415, 198–205. doi:10.1038/415198a
- Bertero, E., and Maack, C. (2018). Calcium signaling and reactive oxygen species in mitochondria. *Circ. Res.* 122, 1460–1478. doi:10.1161/CIRCRESAHA.118.310082
- Beyer, T., Jepsen, L. S., Lüllmann, H., and Ravens, U. (1986). Responses to hypertonic solutions in Guinea-pig atria: Changes in action potentials, force of contraction and calcium content. *J. Mol. Cell. Cardiol.* 18, 81–89. doi:10.1016/S0022-2828(86)80985-3
- Brandes, R., and Bers, D. M. (1999). Analysis of the mechanisms of mitochondrial NADH regulation in cardiac trabeculae. *Biophys. J.* 77, 1666–1682. doi:10.1016/S0006-3495(99)77014-1
- Brandes, R., and Bers, D. M. (2002). Simultaneous measurements of mitochondrial NADH and  $\text{Ca}^{2+}$  during increased work in intact rat heart trabeculae. *Biophys. J.* 83, 587–604. doi:10.1016/S0006-3495(02)75194-1
- Chance, B., and Williams, G. R. (1955). A method for the localization of sites for oxidative phosphorylation. *Nature* 176, 250–254. doi:10.1038/176250A0
- Cortassa, S., Aon, M. A., O'Rourke, B., Jacques, R., Tseng, H. J., Marban, E., et al. (2006). A computational model integrating electrophysiology, contraction, and mitochondrial bioenergetics in the ventricular myocyte. *Biophys. J.* 91, 1564–1589. S0006-3495(06)71867-7 [pii]. doi:10.1529/biophysj.105.076174
- Covian, R., and Balaban, R. S. (2012). Cardiac mitochondrial matrix and respiratory complex protein phosphorylation. *Am. J. Physiol. Hear. Circ. Physiol.* 303, H940–H966. doi:10.1152/ajpheart.00077.2012
- Davoodi, M., Segal, S., Kirschner Peretz, N., Kamoun, D., and Yaniv, Y. (2017). Semi-automated program for analysis of local  $\text{Ca}^{2+}$  spark release with application for classification of heart cell type. *Cell Calcium* 64, 83–90. doi:10.1016/j.ceca.2017.02.003
- De Stefani, D., Raffaello, A., Teardo, E., Szabó, I., and Rizzuto, R. (2011). A forty-kilodalton protein of the inner membrane is the mitochondrial calcium uniporter. *Nature* 476, 336–340. doi:10.1038/NATURE10230
- Dobrev, D., and Nattel, S. (2008). Calcium handling abnormalities in atrial fibrillation as a target for innovative therapeutics. *J. Cardiovasc. Pharmacol.* 52, 293–299. doi:10.1097/FJC.0b013e318171924d
- Dobrev, D., Voigt, N., and Wehrens, X. H. T. (2011). The ryanodine receptor channel as a molecular motif in atrial fibrillation: Pathophysiological and therapeutic implications. *Cardiovasc. Res.* 89, 734–743. doi:10.1093/cvr/cvq324
- Harris, D. A., and Das, A. M. (1991). Control of mitochondrial ATP synthesis in the heart. *Biochem. J.* 280, 561–573. doi:10.1042/BJ2800561
- Kirschner Peretz, N., Segal, S., Arbel-Ganon, L., Ben Jehuda, R., Shemer, Y., Eisen, B., et al. (2017). A method sustaining the bioelectric, biophysical, and bioenergetic function of cultured rabbit atrial cells. *Front. Physiol.* 8, 584. doi:10.3389/fphys.2017.00584
- Komai, H., and Rusy, B. F. (1990). Direct effect of halothane and isoflurane on the function of the sarcoplasmic reticulum in intact rabbit atria. *Anesthesiology* 72, 694–698. doi:10.1097/0000542-199004000-00019
- Liberopoulos, G. (2013). “Production release control: Paced, WIP-based or demand-driven? Revisiting the push/pull and make-to-order/make-to-stock distinctions,” in *Handbook of stochastic models and analysis of manufacturing system operations*. Editors J. M. Smith and B. Tan (New York, NY: Springer New York), 211–247. doi:10.1007/978-1-4614-6777-9\_7

## Funding

The work was supported by ISF 330/19 (YY). The funders had no role in study design, data collection or analysis, decision to publish, or preparation of the manuscript.

## Conflict of interest

The authors declare that the research was conducted in the absence of any commercial or financial relationships that could be construed as a potential conflict of interest.

## Publisher's note

All claims expressed in this article are solely those of the authors and do not necessarily represent those of their affiliated organizations, or those of the publisher, the editors and the reviewers. Any product that may be evaluated in this article, or claim that may be made by its manufacturer, is not guaranteed or endorsed by the publisher.

## Supplementary material

The Supplementary Material for this article can be found online at: <https://www.frontiersin.org/articles/10.3389/fphys.2023.1231259/full#supplementary-material>

- Lindblad, D. S., Murphey, C. R., Clark, J. W., and Giles, W. R. (1996). A model of the action potential and underlying membrane currents in a rabbit atrial cell. *Am. J. Physiol. - Hear. Circ. Physiol.* 271, H1666–H1696. doi:10.1152/ajpheart.1996.271.4.h1666
- Lygate, C. A., Aksentijevic, D., Dawson, D., Ten Hove, M., Phillips, D., De Bono, J. P., et al. (2013). Living without creatine: Unchanged exercise capacity and response to chronic myocardial infarction in creatine-deficient mice. *Circ. Res.* 112, 945–955. doi:10.1161/CIRCRESAHA.112.300725
- Lygate, C. A., Hunyor, I., Medway, D., de Bono, J. P., Dawson, D., Wallis, J., et al. (2009). Cardiac phenotype of mitochondrial creatine kinase knockout mice is modified on a pure C57BL/6 genetic background. *J. Mol. Cell Cardiol.* 46, 93–99. doi:10.1016/j.yjmcc.2008.09.710
- Mason, F. E., Pronto, J. R. D., Alhussini, K., Maack, C., and Voigt, N. (2020). Cellular and mitochondrial mechanisms of atrial fibrillation. *Basic Res. Cardiol.* 115, 72. doi:10.1007/S00395-020-00827-7
- Matsuoka, S., Sarai, N., Jo, H., and Noma, A. (2004). Simulation of ATP metabolism in cardiac excitation–contraction coupling. *Prog. Biophys. Mol. Biol.* 85, 279–299. doi:10.1016/J.PBIOMOLBIO.2004.01.006
- Nguyen, M. H., Dudyca, S. J., and Jafri, M. S. (2007). Effect of Ca<sup>2+</sup> on cardiac mitochondrial energy production is modulated by Na<sup>+</sup> and H<sup>+</sup> dynamics. *Am. J. Physiol. Cell Physiol.* 292, C2004–C2020. doi:10.1152/ajpcell.00271.2006
- Palty, R., Silverman, W. F., Hershfinkel, M., Caporale, T., Sensi, S. L., Parnis, J., et al. (2010). NCLX is an essential component of mitochondrial Na<sup>+</sup>/Ca<sup>2+</sup> exchange. *Proc. Natl. Acad. Sci. U. S. A.* 107, 436–441. doi:10.1073/pnas.0908099107
- Territo, P. R., French, S. A., Dunleavy, M. C., Evans, F. J., and Balaban, R. S. (2001). Calcium activation of heart mitochondrial oxidative phosphorylation: Rapid kinetics of mVO<sub>2</sub>, NADH, and light scattering. *J. Biol. Chem.* 276, 2586–2599. doi:10.1074/JBC.M002923200
- Territo, P. R., Mootha, V. K., French, S. A., and Balaban, R. S. (2000). Ca<sup>2+</sup> activation of heart mitochondrial oxidative phosphorylation: Role of the F(0)/F(1)-ATPase. *Am. J. Physiol. Cell Physiol.* 278, C423–C435. doi:10.1152/ajpcell.2000.278.2.C423
- Verkhratsky, A., Trebak, M., Perocchi, F., Khananashvili, D., and Sekler, I. (2018). Crosslink between calcium and sodium signalling. *Exp. Physiol.* 103, 157–169. doi:10.1113/EP086534
- Voigt, N., Heijman, J., Wang, Q., Chiang, D. Y., Li, N., Karck, M., et al. (2014). Cellular and molecular mechanisms of atrial arrhythmogenesis in patients with paroxysmal atrial fibrillation. *Circulation* 129, 145–156. doi:10.1161/CIRCULATIONAHA.113.006641
- Yang, R., Ernst, P., Song, J., Liu, X. M., Huke, S., Wang, S., et al. (2018). Mitochondrial-mediated oxidative Ca<sup>2+</sup>/calmodulin-dependent kinase II activation induces early afterdepolarizations in Guinea pig cardiomyocytes: An in silico study. *J. Am. Heart Assoc.* 7, e008939. doi:10.1161/JAHA.118.008939
- Yaniv, Y., Juhaszova, M., Lyashkov, A. E. E., Spurgeon, H. A., Sollott, S. J. J., and Lakatta, E. G. G. (2011). Ca<sup>2+</sup>-regulated-cAMP/PKA signaling in cardiac pacemaker cells links ATP supply to demand. *J. Mol. Cell Cardiol.* 51, 740–748. doi:10.1016/j.yjmcc.2011.07.018
- Yaniv, Y., Juhaszova, M., Nuss, H. B. B., Wang, S., Zorov, D. B. B., Lakatta, E. G. G., et al. (2010). Matching ATP supply and demand in mammalian heart *in vivo*, *in vitro*, and *in silico* perspectives. *Anal. Card. Dev. Embryo Old Age* 1188, 133–142. doi:10.1111/j.1749-6632.2009.05093.x
- Yaniv, Y., Sivan, R., and Landesberg, A. (2006). Stability, controllability, and observability of the “four state” model for the sarcomeric control of contraction. *Ann. Biomed. Eng.* 34, 778–789. doi:10.1007/s10439-006-9093-9
- Yaniv, Y., Stanley, W. C., Saidel, G. M., Cabrera, M. E., and Landesberg, A. (2008). The role of Ca<sup>2+</sup> in coupling cardiac metabolism with regulation of contraction: In silico modeling. *Ann. N. Y. Acad. Sci.* 1123, 69–78. 1123/1/69 [pii]. doi:10.1196/annals.1420.009